

Ab initio computational and experimental investigation of the electronic structure of actinide 218 materials

S. Elgazzar,* J. Rusz, and P. M. Oppeneer

Department of Physics and Astronomy, Uppsala University, P.O. Box 516, S-751 20 Uppsala, Sweden

E. Colineau, J.-C. Griveau, N. Magnani, J. Rebizant, and R. Caciuffo

JRC, Institute for Transuranium Elements, European Commission, Postfach 2340, D-76125 Karlsruhe, Germany

(Received 5 February 2010; revised manuscript received 29 April 2010; published 15 June 2010)

We report a comprehensive investigation of the electronic structure and magnetic properties of actinide 218 compounds, which crystallize in the tetragonal Ho_2CoGa_8 crystal structure. Specifically, we study experimentally the group of plutonium-based compounds Pu_2MGa_8 (with $M=\text{Rh}$, Co , and Fe), which are structurally related to the unconventional superconductors PuCoGa_5 and PuRhGa_5 and are measured to be nonmagnetic and nonsuperconducting down to 2 K, yet displaying relatively high linear specific-heat coefficients of 61 to 133 mJ/mol K². We perform density-functional theory based calculations, in which we apply three different approaches to access the tendency of $5f$ electron localization, the local spin-density approximation (LSDA), LSDA+ U , and the $5f$ open-core approach. For comparison to the above-mentioned compounds we also investigate computationally the plutonium compounds with $M=\text{Ir}$ and Pd , the uranium-based compounds U_2MGa_8 (with $M=\text{Co}$, Fe , Rh , and Ru), as well as Np_2CoGa_8 , and Am_2CoGa_8 . On the basis of *ab initio* LSDA calculations we optimize the equilibrium lattice parameters and the internal fractional coordinates within the Ho_2CoGa_8 crystal structure. The obtained lattice parameters are in relatively good agreement with experimental values, when we assume delocalized $5f$ states for all compounds except Am_2CoGa_8 . We discuss the computed electronic structures and the theoretical Fermi surfaces. For the Pu-218 compounds we find that LSDA calculations, in which the $5f$'s are treated as delocalized, predict a magnetically ordered ground state, whereas LSDA+ U calculations predict a nonmagnetic ground state in accordance with experiment. For the U-218 compounds the LSDA itinerant $5f$ approach predicts a nonmagnetic ground state, in accordance with available experimental data. For Am_2CoGa_8 our calculations are consistent with the scenario of localized $5f$ electrons. We find that, on account of the elongated tetragonal structure, most of the theoretical Fermi surfaces are quasi-two-dimensional.

DOI: [10.1103/PhysRevB.81.235117](https://doi.org/10.1103/PhysRevB.81.235117)

PACS number(s): 74.70.-b, 71.28.+d

I. INTRODUCTION

The discovery^{1,2} of d -wave superconductivity in PuCoGa_5 has triggered considerable interest in the electronic properties of PuCoGa_5 and isostructural actinide 115 compounds during the last decade.^{3–12} The peculiar nature of the $5f$ electron shell, which can display both the itinerant character typical of $3d$ electrons and the localized behavior expected for $4f$ electrons, is such that the physical properties of these systems are thought to be governed by the subtle interplay between a variety of different fundamental interactions, thus allowing one to explore links between unconventional superconductivity, magnetism, and non-Fermi liquid behavior in proximity to a quantum critical point.¹³ It must be noticed that, given the complexity of the subject, experimental and theoretical investigations are both required, and very often must be analyzed together to obtain significant results: for example, while no long-range magnetic order is experimentally observed in PuCoGa_5 , the presence of spin polarization and strong magnetic correlations has nonetheless been suggested;² on the other hand, magnetic fluctuations have been proposed as pairing boson for superconductivity,^{14,15} but no ultimate conclusions can be drawn in absence of direct measurements of the relevant spectral densities.¹⁶

Some other actinide-based intermetallic phases have gained much less attention, despite being closely related to

the 115 compounds. One example is the $An_2M\text{Ga}_8$ family of compounds, which crystallize in the tetragonal Ho_2CoGa_8 crystal structure consisting of stacked $M\text{Ga}_2$ and two $An\text{Ga}_3$ layers, as shown in Fig. 1. Only experimental studies on some uranium-based 218 compounds have been published so far,^{17–20} establishing U_2FeGa_8 and U_2RhGa_8 as Pauli paramagnets with a moderately enhanced linear specific heat term γ . Potentially interesting results are expected from investigations of their transuranium analogs, because the transition between the delocalization-localization of $5f$ electrons along the actinide series generally takes place near plutonium.

Previously a similarity between Pu-115 and the earlier discovered^{21–23} Ce-115 unconventional superconductors^{24–26} has been emphasized.^{5,27,28} Ce has one electron in its $4f$ shell and Pu has one hole in its $5f_{5/2}$ shell. Both Ce and Pu unconventional superconductors crystallize in the tetragonal HoCoGa_5 structure, have a proximity to magnetic ordering,^{13,29} exhibit an enhancement of T_c under pressure, and display an identical scaling of T_c with the c/a ratio.^{5,30} Hence, it has been suggested that spin fluctuations could be the unconventional pairing mechanism in both Ce and Pu-115 compounds.^{2,13,28} Apart from the Ce-115's, the Ce-218 compounds have drawn attention.^{31,32} The properties of latter group of materials are very similar to those of the Ce-115's. Ce_2RhIn_8 , for example, displays heavy-fermion behavior,

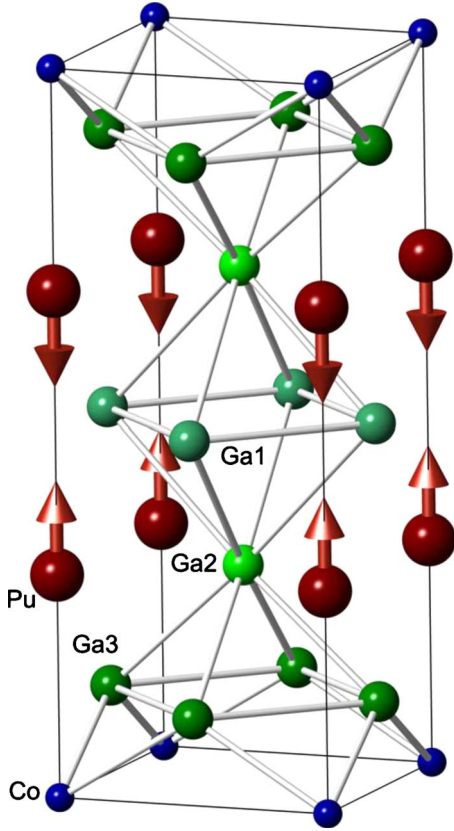


FIG. 1. (Color online) Crystal structure of Pu_2CoGa_8 in the tetragonal Ho_2CoGa_8 structure, showing the labeling of the atoms and the magnetic moments on the actinide atoms in the considered antiferromagnetic arrangement (see text).

magnetic ordering, which makes way for unconventional superconductivity under pressure,³² whereas Ce_2CoGa_8 is a heavy-fermion superconductor at ambient pressure.³¹ The similarities in the physical behavior of the Ce-115's and Pu-115's on the one hand, and the Ce-115's and Ce-218's on the other hand, suggest that the Pu-218's might reveal interesting physical properties, too.

For these reasons we have undertaken a systematic study of the electronic structure, magnetic, and thermal properties of several 218 compounds. The magnetic susceptibility and specific heat of Pu_2RhGa_8 , Pu_2CoGa_8 , and Pu_2FeGa_8 have been experimentally measured, and density-functional theory based calculations have been performed for these and other actinide-based isostructural compounds for comparison.

II. EXPERIMENTAL

Pu_2MGa_8 ($M=\text{Rh}$, Co , and Fe) samples have been grown by the Ga-flux method as described in Ref. 33. The crystals obtained were isolated from the flux and characterized by SEM, EDX, and x-ray diffraction analysis. They were found to be of high quality and crystallizing in the tetragonal Ho_2CoGa_8 crystal structure ($P4/mmm$ space group), with lattice parameters given in Table I. Magnetic susceptibility and specific heat measurements were performed on encapsulated samples to avoid contamination, in a commercial Quan-

TABLE I. Experimentally determined crystallographic, Curie-Weiss, and specific heat parameters for Pu_2MGa_8 compounds ($M=\text{Rh}, \text{Co}, \text{Fe}$). Values are provided per mole Pu where relevant.

	Pu_2RhGa_8	Pu_2CoGa_8	Pu_2FeGa_8
a (Å)	4.316	4.269	4.265
c (Å)	11.144	11.063	11.067
C^* (emu/K)	3.11×10^{-2}	2.41×10^{-2}	0.98×10^{-2}
χ_0^* (emu)	0.22×10^{-3}	0.25×10^{-3}	0.30×10^{-3}
θ_p (K)	-35.7	-58.0	-11.6
μ_{eff} (μ_B)	0.63	0.70	0.38
β (mJ/K ⁴)	0.554	0.100	0.258
γ (mJ/K ²)	133	98	61

tum Design MPMS-7 and PPMS-9 apparatus, under maximum applied magnetic fields of 7 and 9 T, respectively. The measured susceptibility for the Co and Fe compounds (Fig. 2) does not show any magnetic or superconductive transitions down to 2 K; a barely detectable anomaly is present at about 12 K in the Rh-based sample, but nothing can be detected at the same temperature in the specific heat curve. The susceptibility χ for the three compounds displays a paramagneticlike behavior which can be well fitted by a modified Curie-Weiss law of the form³⁴

$$\chi = \chi_0^* + \frac{C^*}{T - \theta_p}, \quad (1)$$

over the whole investigated temperature range; the relevant parameters are listed in Table I. The effective magnetic moment can be calculated by the formula³⁴

$$\mu_{\text{eff}} = \sqrt{\frac{8(C^* - \theta_p \chi_0^*)^2}{C^*}} \quad (2)$$

and is in all cases reduced (slightly but significantly for $M=\text{Rh}$ and Co , more strongly for $M=\text{Fe}$) with respect to the

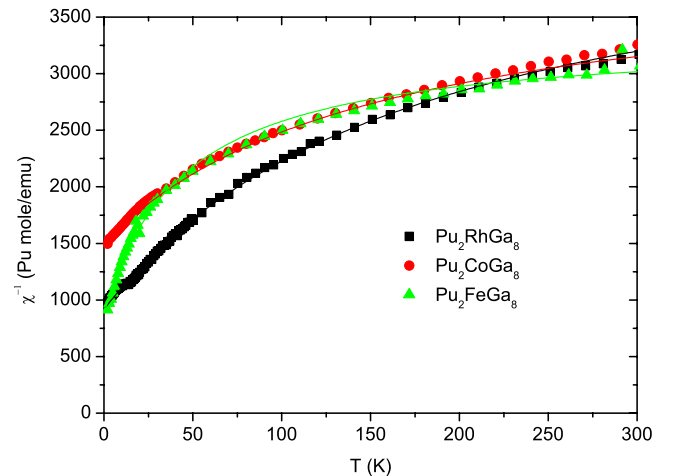


FIG. 2. (Color online) Inverse magnetic susceptibility measured (with an applied magnetic field of 7 T) for the Pu_2MGa_8 compounds (see legend). Lines are fits to the modified Curie-Weiss law given in Eq. (1).

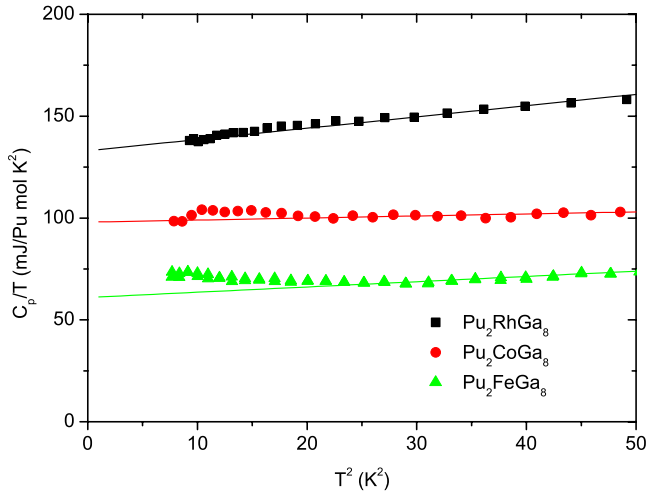


FIG. 3. (Color online) Results of low-temperature specific heat measurements for Pu_2MGa_8 compounds (see legend), given as a C_p/T vs T^2 plot. Lines are linear fits to Eq. (3).

effective moment value for free Pu^{3+} ions. The reduction could be due to a partially delocalized character of the $5f$ electrons or it could be caused by the crystal field. The possible valency of Pu in several Pu-compounds has been discussed^{35–37} previously in terms of trivalent or divalent Pu. For the nonmagnetic Pu^{2+} ion the Curie-Weiss behavior of the susceptibility would vanish, but this we do not observe in Fig. 2, even though there is a deviation of χ for Pu_2FeGa_8 . The Curie-Weiss behavior is compatible with the assumption that the actinide ions are trivalent (as in the parent 1:1:5 phases). Despite the absence of any transition to an ordered state, the relatively large negative values of the paramagnetic Curie temperature θ_p allow to infer that a significant antiferromagnetic exchange interaction is present in these compounds.

Specific heat measurements for the three compounds were virtually unaffected by the magnetic field, and also in this case no transitions were revealed, although a small anomaly of unknown origin is visible at low temperatures. Figure 3 shows the low-temperature part, which can be expressed as³⁸

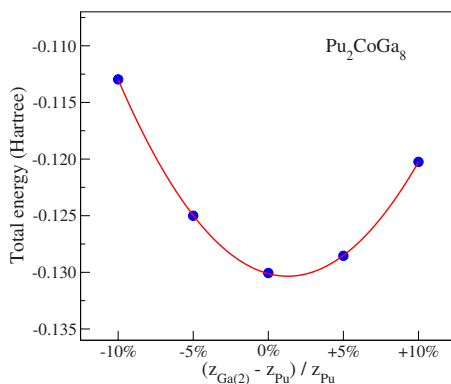


FIG. 4. (Color online) Optimization of the fractional z -coordinate (dimensionless) of Ga(2) with respect to the z -coordinate of Pu atom in Pu_2CoGa_8 .

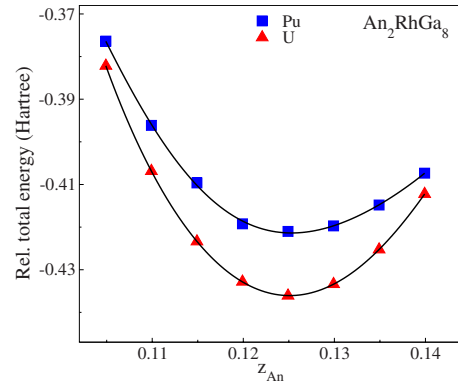


FIG. 5. (Color online) Simultaneous optimization of the fractional z -coordinate (dimensionless) of the actinide layer and of Ga(2) in U_2RhGa_8 and Pu_2RhGa_8 .

$$C_p = \gamma T + \beta T^3. \quad (3)$$

The obtained values of the Sommerfeld coefficient γ (Table I) suggest that these compounds can be classified as moderately enhanced heavy fermion systems. We note that whereas fitting the T^2 dependence of C_p/T works reasonably well for Pu_2RhGa_8 and Pu_2CoGa_8 , there is a deviation from linearity at low temperatures for Pu_2FeGa_8 , which corroborates with its different susceptibility behavior. The origin of this deviation is currently unknown, but it could be an indication of the presence of magnetic states near to the ground state. The γ coefficient of Pu_2FeGa_8 has therefore a larger uncertainty.

Several other An_2MGa_8 compounds, viz. Pu_2PdGa_8 , Pu_2IrGa_8 , Np_2CoGa_8 , and Am_2CoGa_8 , were prepared previously.³⁹ Their lattice parameters were determined,³⁹ but the physical properties of these 218-materials have not been classified in more detail.

III. COMPUTATIONAL METHODS

A. Electronic structure calculations

The majority of our calculations was performed using the relativistic version^{40,41} of the full-potential local orbital (FPLO) minimum-basis band-structure method.⁴² In this scheme the four-component Kohn-Sham-Dirac equation, which implicitly contains spin-orbit coupling up to all orders, is solved self-consistently.

For the present calculations, we used the following basis sets: for U, Np, and Pu the $5f$; $6s6p6d$; $7s7p$ states were chosen as valence states while for Am the $5f$ states are treated as core states. This is an approximation, because the Am $5f$ states do not completely vanish in the interstitial region. For Fe and Co we used the $3d$; $4s4p$ states and equivalent sets with higher quantum numbers for Ru, Rh, Pd, and Ir, while for Ga we used $3d$; $4s4p4d$. For the actinides the high-lying $6s$ and $6p$ semicore states are included in the basis. These semicore states have non-negligible tails reaching the interstitial region or even other atomic spheres. The site-centered potentials and densities were expanded in spherical harmonic contributions up to $l_{\text{max}}=12$. The number of \mathbf{k} -points in the irreducible part of the Brillouin zone was 196, but calculations were made also with 405 and up to 2176

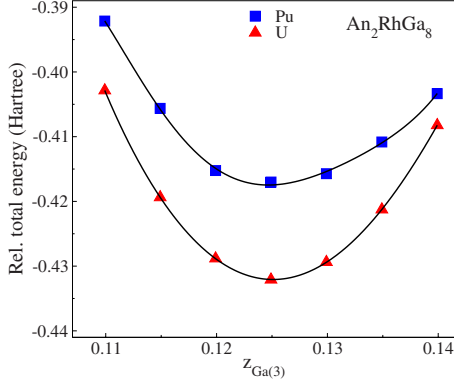


FIG. 6. (Color online) Optimization of the fractional z -coordinate (dimensionless) of the Ga(3) layer in U_2RhGa_8 and Pu_2RhGa_8 .

k -points to resolve the density of states at the Fermi energy (E_F). The Perdew-Wang⁴³ parameterization of the exchange-correlation potential in the local spin-density approximation (LSDA) was used.

Selected systems were also calculated with the WIEN2K code.⁴⁴ The spin-orbital interaction was included in the second variational step (see Ref. 45), and the relativistic local orbitals extension⁴⁶ was used. We have employed the orbital-dependent LSDA+ U method with around mean-field double-counting correction,⁴⁷ which correctly reproduced the nonmagnetic ground state of δ -Pu or Pu-115 systems.^{48,49} The muffin-tin radii were set to 2.9, 2.6, and 2.1 Bohr radii for the actinide, transition metal, and Ga, respectively. The basis size was determined by the $RK_{\max}=8.0$ parameter, which led to *ca* 1400 basis functions per formula unit. Furthermore, we used 720 k -points in the irreducible wedge of the first Brillouin zone (BZ).

B. Structural optimization

The Ho_2CoGa_8 crystal structure in which the An_2MGa_8 compounds crystallize is characterized by a stacking of MGa_2 and $AnGa_3$ layers, see Fig. 1. The An_2MGa_8 ($An=Pu$,

U, Np, and Am, $M=Co$, Rh, Ir, Fe, and Pd) have in this respect a structural similarity with the An-115 compounds where the tetragonal structure consists of MGa_2 and $AnGa_3$ layers, stacked along the c axis. The unit cell of the An-115 tetragonal structure can in turn be viewed as derived from the cubic $AnGa_3$ unit cell, which has been elongated along the c axis by an extra layer of MGa_2 being built in. The unit cell of An-218 structure can then be derived from that of the An-115 structure by adding an additional $AnGa_3$ layer, see Fig. 1.

The unit cell has three internal structure parameters, namely the z -coordinate of the actinide element, z_{An} , and the z -coordinates of the two nonequivalent Ga positions [Ga(2) and Ga(3) in Fig. 1]. Since these structure parameters are not yet known from experiments, we have calculated them by total energy minimization. The structural optimization was performed using the FPLO code. We have not performed full relaxations of all free parameters in these structures, rather we have performed the following steps: First we kept the lattice parameters a and c fixed at experimentally known values,³⁹ see also Table I. Then, at fixed positions of the actinide layer and Ga(3) layer we have varied the z coordinate of Ga(2) atom. Results of this optimization are presented in Fig. 4. It turns out that there is a rather broad total energy minimum, with a $z_{Ga(2)}$ which is centered almost precisely around the z_{An} position of the actinide layer. Therefore in all subsequent optimizations we have assumed that $z_{An}=z_{Ga(2)}$. In the next step we have simultaneously optimized the z -coordinate of the actinide and Ga(2) atoms at a fixed position of the Ga(3) layer, see Fig. 5. In the last step of optimization of internal parameters we have varied the position of the Ga(3) layer (see Fig. 6), keeping the actinide and Ga(2) at their optimized positions from the previous step. Finally, with the optimized internal parameters we have relaxed the lattice constants. This procedure was in addition carried out adopting several possible magnetic phases for the plutonium based 218 compounds. We have considered the paramagnetic (PM) phase, the ferromagnetic phase (FM), as well as an antiferromagnetic (AFM) phase that is consistent with the crystal structure unit cell (see Fig. 1). The summary of optimized and experimental structure parameters is presented in Table II.

TABLE II. Experimental lattice parameters a and c (from this work, Refs. 18, 19, and 39), ratio of theoretical and experimental unit cell volumes V_{th}/V_{exp} and calculated internal structure parameters z_{An} and $z_{Ga(3)}$ (see text) of the studied An-218 compounds.

Compound	$a_{exp}/\text{\AA}$	$c_{exp}/\text{\AA}$	V_{th}/V_{exp}	z_{An}	$z_{Ga(3)}$
Pu_2CoGa_8	4.269	11.063	0.919	0.3058	0.1188
Pu_2RhGa_8	4.316	11.144	0.939	0.3070	0.1264
Pu_2IrGa_8	4.322	11.102	0.928	0.3053	0.1259
Pu_2FeGa_8	4.265	11.067	0.912	0.3055	0.1194
Pu_2PdGa_8	4.309	11.217	0.919	0.3083	0.1274
U_2FeGa_8	4.256	10.980	0.935	0.3053	0.1182
U_2RhGa_8	4.297	11.080	0.943	0.3095	0.1249
U_2RuGa_8	4.288	11.062	0.959	0.3068	0.1233
Np_2CoGa_8	4.251	11.021	0.916	0.3078	0.1194
Am_2CoGa_8	4.256	11.165	0.907	0.3075	0.1203

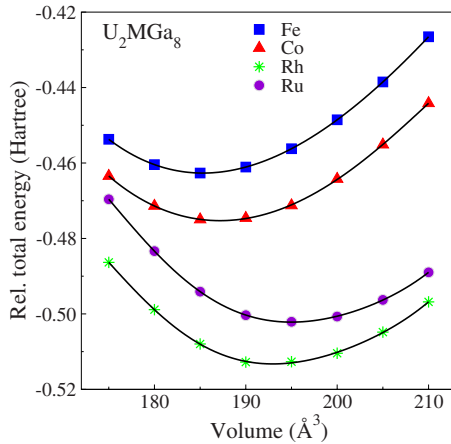


FIG. 7. (Color online) Optimization of the unit cell volume of the U_2MGa_8 compounds ($M=Fe, Co, Rh,$ and Ru). The total energy for each individual system has been shifted by a constant value to bring all energies to a common energy range.

IV. URANIUM 218 COMPOUNDS

The uranium compounds U_2MGa_8 with $M=Fe, Rh,$ and Ru were studied experimentally.^{17–20} For all three compounds no signs of a magnetic phase transition were detected, despite the fact that the U–U nearest-neighbor distances in all these compounds are well beyond the Hill limit. The electronic specific heat γ coefficient is relatively low for these $5f$ -itinerant compounds, and there is no Curie-Weiss behavior up to a few hundred Kelvins,¹⁸ suggesting rather wide uranium $5f$ bands. We have calculated their electronic structures, including the related $M=Co$ compound, for which so far only structural data exist.⁵⁰ In the following paragraphs, we present a detailed account of our theoretical results.

All studied U-218 compounds have converged to a non-magnetic state, in agreement with experimental observations. The energy vs. unit cell volume curves are shown in Fig. 7. In agreement with available experiments, we obtain that the unit cell volume of systems with the $4d$ transitional metals Rh and Ru is larger than that of their $3d$ counterparts Fe and Co . In general, the theoretical unit cell volumes agree with the experimental ones within 7%, which is a slight overbinding typical for LSDA density-functional theory calculations.

A concise picture of their electronic structure can be obtained from the plots of their density of states (DOS), Fig. 8. There we compare the converged paramagnetic DOS of the studied U-218 systems. These are all closely related. The dominant contribution to the DOS at the Fermi level comes from uranium $5f$ states, particularly from the almost 2 eV wide $5f_{5/2}$ band, which has a relatively long tail toward higher binding energies. This is in accord with experimental observations of medium-high-specific heat γ coefficients 52, 43, and 57 $mJ K^{-2}$ per mole of uranium for U_2FeGa_8 , U_2RhGa_8 , and U_2RuGa_8 , respectively.^{18,19} The theoretical values for the unenhanced specific heat are 20, 19, and 15 $mJ K^{-2}/mol U$, and 21 $mJ K^{-2}/mol U$ for U_2CoGa_8 , respectively. These results indicate a modest many-body enhancement of the DOS at Fermi level. The Fermi level in all

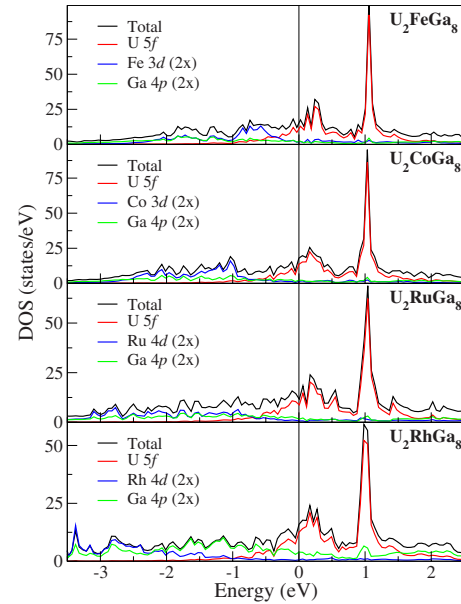


FIG. 8. (Color online) Density of states of the U_2MGa_8 compounds (with $M=Fe, Co, Rh,$ and Ru). For each compound the panel contains the total DOS, DOS of U- $5f$ states, DOS of M - d states, and DOS of Ga- $4p$ states (per formula unit). To enhance visibility, the DOS of M - d states and Ga- $4p$ states were multiplied by two.

four systems is inside or close to a local minimum of the DOS, which is caused by hybridization effects. It is not due to the spin-orbit splitting of the $5f$ band into $5f_{5/2}$ and $5f_{7/2}$ sub-bands—that occurs approximately 0.75 eV above the Fermi level. The $5f_{7/2}$ bands in all studied U-218 systems form a narrow peak centered 1 eV above the Fermi level. A second large contribution to the DOS comes from the transition metal $3d$ or $4d$ states. These form a 2–3 eV wide band, which is almost completely below the Fermi level for the Fe and Co $3d$ transition metals, while for Rh and Ru $4d$ metals its main part is 2 eV and more below the Fermi level. The d band of the transition metals does not seem to hybridize much with the U $5f$ bands, which is probably due to their limited spatial extent and presence of the separating Ga layer. Finally, the summed Ga $4p$ band is a wide, almost featureless band, which shows signs of hybridization with both the U- $5f$ band and M - d bands. Despite its width, owing to the eightfold multiplicity of Ga per formula unit, its contribution to the DOS at the Fermi level is comparable to the DOS of the transition metal, contributing thus to the calculated γ coefficient.

A more detailed picture of the electronic structure at the Fermi level can be inspected from the plot of the band structure. In Fig. 9, we show, for sake of brevity, only the calculated bandstructure of U_2FeGa_8 . The fatness of bands in Fig. 9 indicates the amount of uranium $5f_{5/2}$ character (red color), amount of the almost unoccupied uranium $5f_{7/2}$ character (blue color) and iron $3d$ character, which are almost fully occupied (green color). The DOS around the Fermi level is dominated by the uranium $5f_{5/2}$ states. There are in total four bands which cross the Fermi level. The corresponding four Fermi surface sheets are shown in Fig. 10. Two of them have

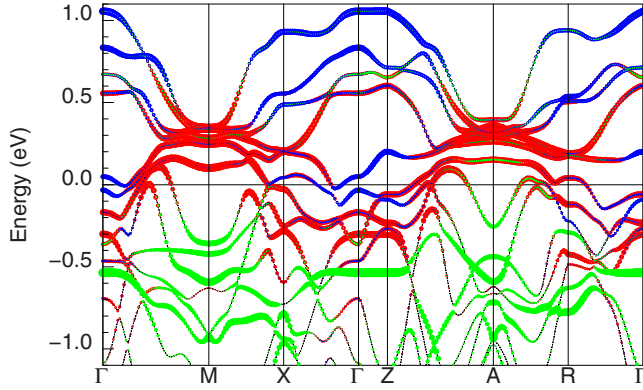


FIG. 9. (Color online) Calculated bandstructure of U_2FeGa_8 . The thickness of the bands is proportional to the character of the bands: blue, red, and green denote $U-5f_{7/2}$, $U-5f_{5/2}$, and $Fe-3d$ characters, respectively.

a rather two-dimensional character, but the other two rather small sheets, despite the very short c^* axis, are three dimensional.

U_2RuGa_8 also has four Fermi surface sheets with a similar topology. For U_2RhGa_8 and U_2CoGa_8 there are only three bands crossing the Fermi level. Due to the band filling, the small Fermi surface pockets disappear and also the four tubular Fermi surface sheets (Fig. 10) become smaller and rounder. Compared to the small Fermi surface of $UCoGa_5$ (Ref. 51), the Fermi surface sheets of U_2CoGa_8 and U_2RhGa_8 are distinctly larger, which can be explained by a delicate band filling in $UCoGa_5$. They are also more two dimensional than those of the parent compound UGa_3 (Ref. 52) and of $UCoGa_5$ (Ref. 51).

V. PLUTONIUM 218 COMPOUNDS

Our experimental analyses from Sec. II do not indicate any phase transitions down to 2 K, which makes the Pu-218's different from their Pu-115 counterparts. Nevertheless, using the modified Curie-Weiss law we obtained indications

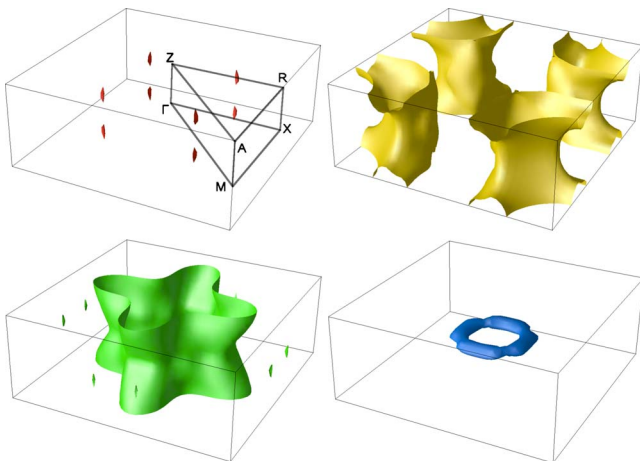


FIG. 10. (Color online) Fermi surface of U_2FeGa_8 , calculated with the LSDA approach. The labeling of the high-symmetry points is shown in the top-left panel.

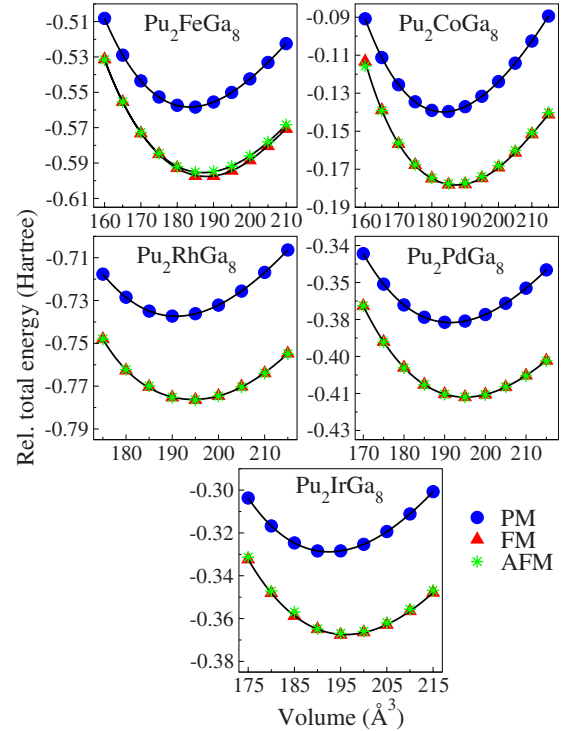


FIG. 11. (Color online) Optimization of the unit cell volume of the Pu_2MGa_8 compounds ($M=Fe, Co, Rh, Pd,$ and Ir), assuming paramagnetic (PM), ferromagnetic (FM), or antiferromagnetic (AFM) order, respectively.

of antiferromagnetic exchange interactions leading to negative Néel temperatures.

We have evaluated the energy versus unit cell volume dependence for the PM, FM, and AFM states. These are shown together in Fig. 11 for all studied systems. Contrary to the uranium 218 compounds, the LSDA total energy of the Pu-218's is lower for the magnetically ordered state. An interesting observation is that the total energies for the FM and AFM state almost coincide. From this we can conclude that (i) there is a stronger tendency toward magnetism in Pu-218 compounds compared to U-218 compounds, and (ii) the interlayer exchange coupling between Pu atoms is of negligible size. The second observation can be reformulated in the following way: if there would be a magnetic ground state in the Pu-218 compounds, then it would most likely not be the FM or AFM state studied here, but some more complicated arrangement of magnetic moments. The magnetic unit cell would consequently be larger than the here-used elementary cell of the crystal structure. Due to weak interlayer coupling it can be expected that thermal fluctuations would easily destroy a long-range magnetic order. New experiments at lower temperatures will hopefully shed more light on this question. Note that the weak interlayer coupling is in accord with the expected two dimensionality of the system, at least from the magnetic interactions point of view.

In the following part, we focus on the nonmagnetic calculations. The calculated DOS of all studied Pu-218 compounds is summarized in Figs. 12 and 13. A feature common to all five systems is the placement of the Pu $5f$ states. The spin-orbit interaction splits the $5f$ band into two sub-bands,

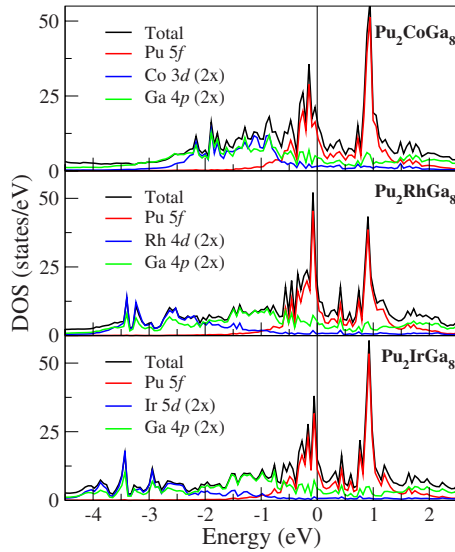


FIG. 12. (Color online) Calculated density of states of nonmagnetic Pu_2MGa_8 compounds ($M=\text{Co}$, Rh , and Ir). For each compound the plot contains the total DOS, partial DOS of the $\text{Pu-}5f$ states, DOS of M - d states, and DOS of $\text{Ga-}4p$ states (per formula unit). To enhance visibility, the DOS of the M - d states and $\text{Ga-}4p$ states were multiplied by two.

$5f_{5/2}$ and $5f_{7/2}$, which are separated by approximately 1 eV. The $5f_{5/2}$ band is almost fully occupied and its major part lies approximately 0.5 eV below the Fermi level. The DOS at the Fermi level consists thus mainly of $\text{Pu } 5f$ character, though the total DOS at E_F it is not very large. At the Fermi level a non-negligible contribution comes from $\text{Ga } 4p$ bands, which strongly hybridize with d bands of the transition metals. The position of the d -band varies for the different elements. For $\text{Pu-}218$ systems with $3d$ transition metals (Fe and Co) the $3d$ states form an almost 2 eV wide band placed nearly entirely below the Fermi level with just a weak tail at higher energies. For the $4d$ and $5d$ elements, the d -band lies 2 eV or more below the Fermi level and is typically narrower. E.g., for Pu_2PdGa_8 it is centered around -4 eV and

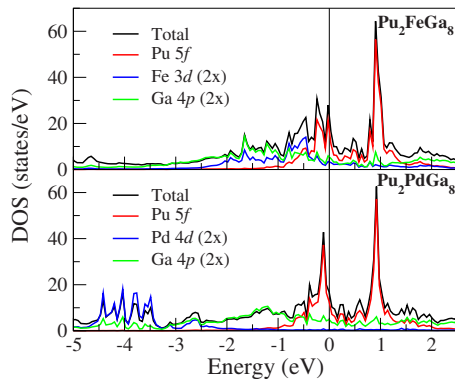


FIG. 13. (Color online) Density of states of nonmagnetic Pu_2MGa_8 compounds, with $M=\text{Fe}$ or Pd . For each compound the plot contains the total DOS, DOS of $\text{Pu-}5f$ states, DOS of M - d states, and DOS of $\text{Ga-}4p$ states (per formula unit). To enhance visibility, the DOS of M - d states and $\text{Ga-}4p$ states were multiplied by two.

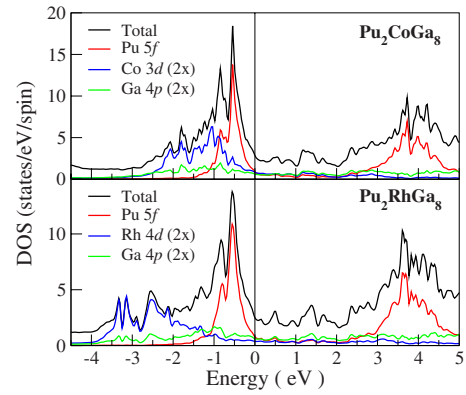


FIG. 14. (Color online) Density of states of Pu_2CoGa_8 and Pu_2RhGa_8 compounds calculated using the $\text{LSDA}+U$ exchange-correlation potential, with $U=3$ eV and $J=0.6$ eV). For each compound the plot contains total DOS, DOS of the $\text{Pu-}5f$ states, DOS of Co or $\text{Rh } d$ states, and DOS of the $\text{Ga-}4p$ states (per formula unit). To enhance visibility, the DOS of the d states and $\text{Ga-}4p$ states was multiplied by two.

only about 1 eV wide. We note that Pu_2FeGa_8 behaves differently from the other systems, as it has a $5f$ peak just at the Fermi level and as a consequence a high DOS at the Fermi level. The computed, unenhanced specific heat coefficients of Pu_2CoGa_8 , Pu_2RhGa_8 , and Pu_2FeGa_8 are 24, 35, and 31 mJ K^{-2} per mole Pu , respectively. These are a factor of two to four smaller than the experimental values given in Table I.

A natural question from the theoretical point of view would be, whether the suggested magnetic ground state is in fact not a consequence of a failure of the LSDA exchange-correlation potential. This has indeed been concluded for some Pu compounds, including $\delta\text{-Pu}$,⁴⁸ the Pu monochalcogenides,⁵³ and the related $\text{Pu-}115$ compounds.⁴⁹ This has been explained from the fact that the $\text{LSDA}+U$ approach favors stronger the j - j coupling limit, which leads to a nearly filled, nonmagnetic $5f_{5/2}$ subshell.^{48,49} We have therefore also performed around-mean field (AMF) $\text{LSDA}+U$ calculations with $U=3$ eV and $J=0.6$ eV for Pu_2CoGa_8 and Pu_2RhGa_8 systems, at the experimental structure parameters. This value of the Coulomb U gave previously improved results for several Pu compounds, including the related PuCoGa_5 ,^{9,49,53,54} The $\text{LSDA}+U$ calculations with this U value indeed converged to a nonmagnetic ground state. The $\text{LSDA}+U$ potential has quite dramatic effects on the $\text{Pu } 5f$ bands, Fig. 14. First, the on-site Coulomb correlations have enlarged the splitting of the $5f_{5/2}$ and $5f_{7/2}$ sub-bands to 4 eV, which corresponds to the sum of on-site Coulomb term $U=3$ eV and the spin-orbit interaction strength of 1 eV (see above). Second, the bands have become wider due to an enhanced on-site repulsion, exchange interaction, and some hybridization. The $5f_{5/2}$ band, which was only about 0.5 eV wide in the LSDA calculation, is now almost 1 eV wide. The unoccupied $5f_{7/2}$ band, centered about 3.5 eV above the Fermi level, is more than 1.5 eV wide. The broadening of the $5f_{5/2}$ band and its slight downwards energy shift results in a much lower predicted DOS at the Fermi level. The majority of the DOS at the Fermi level corresponds in the LSDA

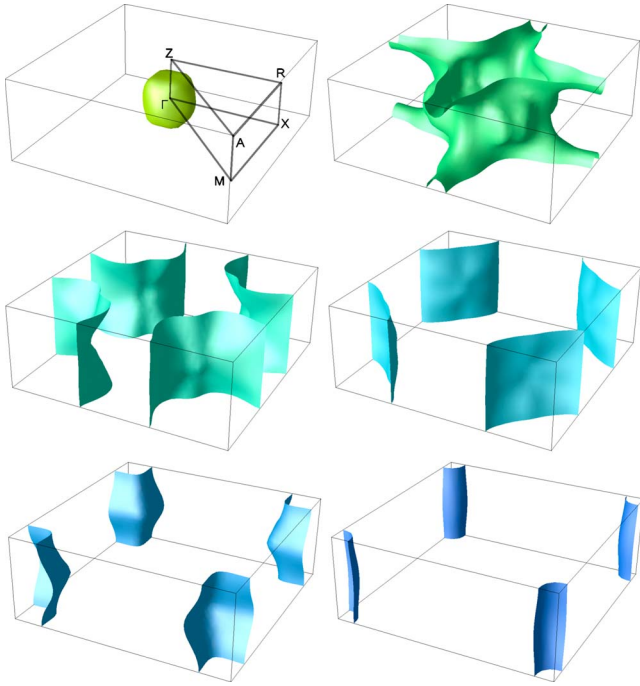


FIG. 15. (Color online) Fermi surface topology of Pu_2CoGa_8 calculated using the LSDA+ U exchange-correlation potential.

+ U calculation to interstitial states, i.e., to highly delocalized electrons. Note that while the LSDA+ U method arguably improves the description of the strongly correlated $5f$ bands, it is still a static method, i.e., it does not describe quantum fluctuations. Particularly, it cannot capture the quasiparticle peak, which can be expected to form at the Fermi level as a manifestation of many-particle correlation effects. This is, for instance, very important for reliable predictions of the electronic specific heat coefficient. To capture the physics of these phenomena one needs to go beyond the LSDA+ U method, e.g., by means of dynamical mean-field theory approaches.^{55,56} In this sense our LSDA and LSDA+ U calculations should be taken as a starting point for understanding these complex materials, and the specific heat coefficients calculated by LSDA or LSDA+ U can serve as an estimation of the strength of the many-body effects, when compared to the available experimental values.

Using the LSDA+ U approach, we have also calculated the Fermi surface of Pu_2CoGa_8 , shown in Fig. 15. Different from the nonmagnetic local-density approximation calculations, in the LSDA+ U result we observe 6 bands crossing the Fermi level, Fig. 16. The lowest one leads to a small hole surface with volume only for 0.02 states and the highest band forms a small electron sheet with similar volume. Most of the bands—corresponding to the four bands with highest band number—are very two dimensional. Conversely, the two lowest bands show distinct three-dimensional features. The lowest band forms a small hole sheet that has an almost spherical Γ -centered shape. I.e., its de Haas-van Alphen frequency should be largely direction independent. The second lowest band has a much more complicated topology. A previous LSDA+ U calculation⁵⁴ for the Pu-115 compounds also revealed a rather two-dimensional Fermi surface, yet with as

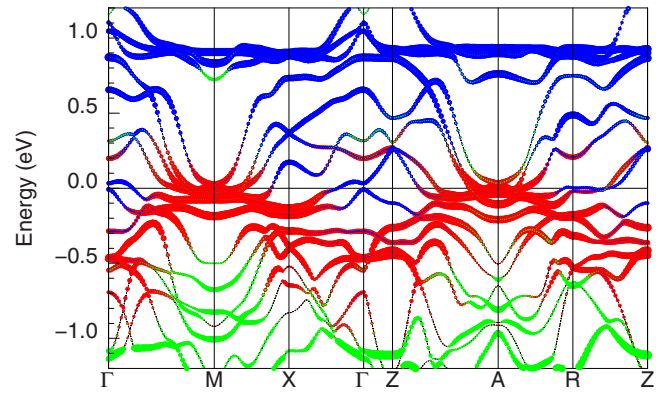


FIG. 16. (Color online) Bandstructure of nonmagnetic Pu_2CoGa_8 within the LSDA. Thickness of the bands is proportional to the character of the bands: blue, red and green denote $\text{Pu-}5f_{7/2}$, $\text{Pu-}5f_{5/2}$, and $\text{Co-}3d$ characters, respectively.

well two Fermi surface sheets that are more three-dimensional, one of these being a small spherical surface very similar to the one shown in Fig. 15.

The appearance of the three-dimensional features can be qualitatively explained in the following way. Both families of actinide intermetallic compounds—the An-115's and An-218's—can be derived from a parent compound AnGa_3 , which has a face-centered cubic crystal structure. The An-115 compounds can be formed by inserting an MGa_2 layer between two AnGa_3 layers, while An-218 compounds are formed by alternating two layers of AnGa_3 with one layer of MGa_2 . In this sense, the An-218 compounds are somewhat closer to the parent compound, which has a fully three-dimensional Fermi surface topology.^{57,58}

VI. NEPTUNIUM AND AMERICIUM 218 COMPOUNDS

The uranium 218 compounds turned out to be nonmagnetic, despite the expectations based on Hill criterion. For the plutonium compounds there are no proofs of magnetism. The Pu-115 counterparts are nonmagnetic. Nonetheless, we have seen that plutonium 218 compounds appear to have a certain tendency toward a formation of the magnetic moment, also demonstrated by non-negligible antiferromagnetic exchange interactions indicated by negative Néel temperatures and our LSDA calculations.

Neptunium lies between the uranium and plutonium in the Periodic Table. Given the itinerant nature of $5f$ electrons in the U-218 compounds on one side and the complicated electron-electron correlations in Pu-218 compounds on the other side, *a priori* there does not emerge any clear picture for what should be the electronic and magnetic structure of the neptunium 218 compounds. For the related NpCoGa_5 compound both LSDA calculations and experiments give that it orders antiferromagnetically.^{7,51,59,60} By performing a paramagnetic calculation for Np_2CoGa_8 (not shown) we observe that a sharp peak develops directly at the Fermi level. Such a high-DOS peak usually indicates an instability that can be removed by a symmetry breaking, for example, magnetic ordering. Indeed, the DOS at E_F turns out to be much reduced for the AFM and FM phases. The exchange splitting

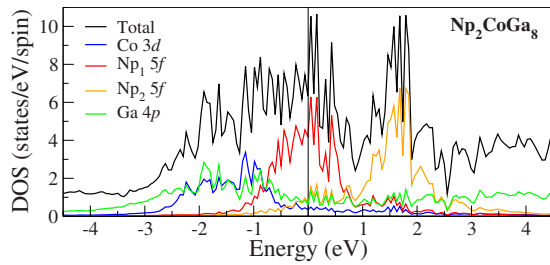


FIG. 17. (Color online) Spin-up DOS of antiferromagnetic Np_2CoGa_8 . Note the spin-splitting of the two neptunium atoms with opposite magnetic moment orientations. The spin-down DOS (not shown) has identical features, only the role of the two neptunium atoms is interchanged.

of the Np $5f$ states pushes a part of the $5f$ DOS for a selected spin orientation to higher binding energies, while the opposite-spin DOS is shifted above E_F , see Fig. 17. We observe only one band crossing the Fermi energy along the high-symmetry lines. In both studied magnetic phases the contribution of the Np $5f$'s dominates the DOS in the vicinity of E_F .

The total energy of the AFM and FM phases is lower than the total energy of the PM phase, thus favoring a magnetically ordered ground state. The total energies of the AFM and FM phases are computed to be very close, with the FM phase being slightly deeper. However, we note that there could possibly exist other magnetically ordered phases different from the ones that we consider here (cf. Fig. 1). For the related Np-115 compounds a very rich magnetic phase diagram has been revealed, consisting of several noncollinear AFM and FM phases.^{7,60,61} Similar experimental studies would be required for Np_2CoGa_8 to address this issue comprehensively, but these have not yet been performed. The unenhanced linear specific-heat coefficient, calculated for the PM and AFM phase, is $\gamma=68$ and $\gamma=30$ mJ/mol K^2 , respectively.

Americium is typically nonmagnetic, since in most compounds it has six $5f$ electrons, which fully occupy the $5f_{5/2}$ levels that are separated from the unoccupied $5f_{7/2}$ levels by a strong spin-orbit interaction. The $5f_{5/2}$ levels are usually located a few electron volts below the Fermi level and thus do not contribute to the Fermi surface topology. On the other hand, the $5f_{7/2}$ are empty and located a few eV above the Fermi level. This typical situation, which originates from the strong spin-orbit interaction leading to $j-j$ coupling for the Am atom, is not correctly described by the LSDA, which places the $5f$ shell typically in the vicinity of the Fermi level. Therefore, we have employed the LSDA+ U approach and an open- f -core treatment for the Am_2CoGa_8 compound. In the open-core approximation the $5f$ electrons are treated as core states, which means that the hybridization of $5f$ electrons with other valence states is neglected. The open-core calculation leads to a nonmagnetic state, mainly because the $5f_{5/2}$ shell is fully occupied. In the LSDA+ U approach the splitting between $5f_{5/2}$ and $5f_{7/2}$ is strengthened by the on-site Coulomb repulsion and as a result, the $5f_{5/2}$ are fully occupied, while $5f_{7/2}$ are empty—in accord with the open-core calculation. Thus in both approaches the $5f$ states are re-

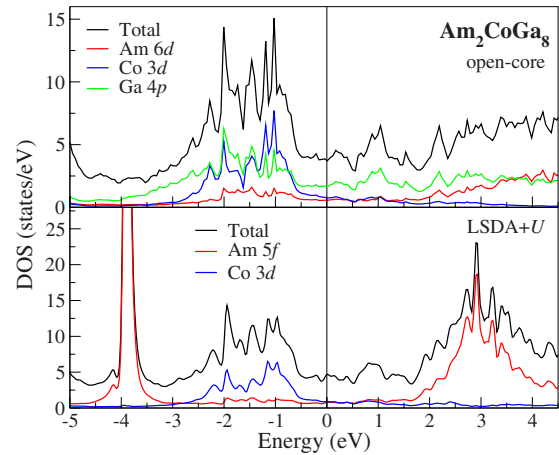


FIG. 18. (Color online) Paramagnetic DOS of Am_2CoGa_8 calculated using the open-core treatment (top) and LSDA+ U approach with $U=5$ eV, $J=0.6$ eV (bottom) for the americium $5f$ states. Note the different scale on the vertical axes. The peak $5f$ DOS of the LSDA+ U calculation around -4 eV in the bottom panel is approximately 60 states/eV high.

moved from the valence region, and both lead to a nonmagnetic ground state and a very similar DOS in the vicinity of the Fermi level, see Fig. 18. The similarity of the DOS surrounding the Fermi level in both calculations,⁶² confirms that the $5f$ states do not influence the Fermi surface topology. It is also an indirect proof of the validity of open-core approximation for the electronic structure near to the Fermi level. The LSDA+ U calculation with $U=5$ eV reveals a narrow $5f_{5/2}$ peak at 4 eV below the Fermi level. The $5f_{7/2}$ states form a somewhat broader band approximately 3 eV above the Fermi level. At the Fermi level the DOS is dominated by itinerant Ga p states. We have verified that a different value of U does not change the DOS in the vicinity of the Fermi level, it only shifts the centers of gravity of the $5f_{5/2}$ and $5f_{7/2}$ bands. The Fermi surface topology obtained from the LSDA+ U calculation (and from the f -core approach), Fig. 19, is remarkably similar to the theoretical FS topology of the related isoelectronic La_2RhIn_8 compound,⁶³ which has no f electrons. The authors of Ref. 63 have concluded, on the base of de Haas-van Alphen experiments, that the Fermi surface topologies of La_2RhIn_8 and Ce_2RhIn_8 are very similar, evidencing the localized Ce $4f$ character of Ce_2RhIn_8 . We obtain here that this similarity extends also to Am_2CoGa_8 ; $5f$ localization leads to a Fermi surface derived mainly from the Co and Ga bonding in the Ho_2CoGa_8 unit cell.

VII. CONCLUSIONS

We have performed a comprehensive experimental and theoretical investigation of Pu-based 218 compounds. Pu_2RhGa_8 , Pu_2CoGa_8 , and Pu_2FeGa_8 are paramagnetic in the whole investigated temperature range. The relatively large values of γ obtained for the Pu-based compounds from low-temperature specific-heat measurements allow to classify these compounds as moderately enhanced heavy fermion systems. Despite the absence of magnetic ordering, the pres-

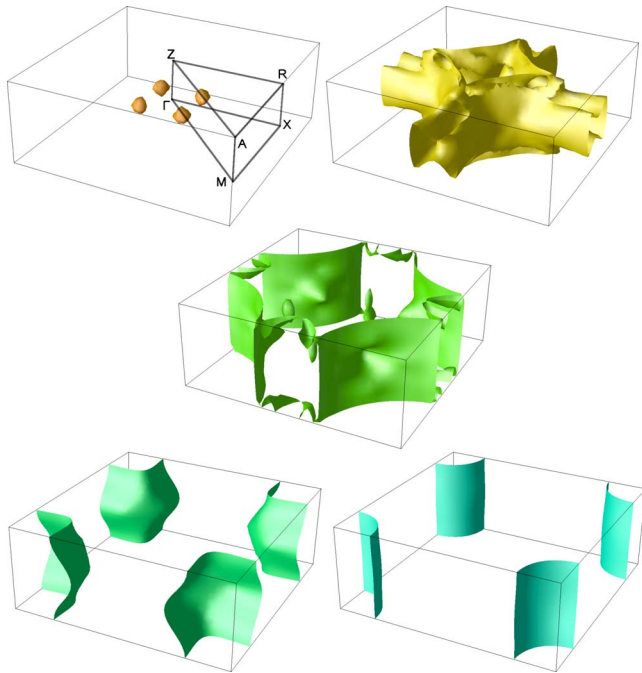


FIG. 19. (Color online) Fermi surface of Am_2CoGa_8 calculated using the LSDA+ U approach.

ence of strong magnetic correlations are suggested by the large negative value of the Curie-Weiss temperature. According to our first-principles LSDA calculations, however, the antiferromagnetic and ferromagnetic structures are very close in energy, indicating that there is only a weak interlayer coupling between the actinide layers. More complicated antiferromagnetic arrangements may yet need to be studied to get better insight into the nature of the antiferromagnetic exchange interaction indicated by the above-mentioned data. As the Pu $5f$ states in the 218 compounds are expected to be on the verge of the $5f$ delocalized to localized transition, we have in addition employed the LSDA+ U approach to treat a moderate degree of Pu $5f$ localization. The LSDA+ U approach predicts a nonmagnetic ground state for the investigated Pu 218-compounds. Further investigations are consequently required to decide which exchange-correlation functional provides the best results for the Pu-218 compounds. The fact that the effective magnetic moment is slightly reduced with respect to the free Pu^{3+} one suggest that at least a partial localization of the $5f$ electrons is occurring. This is not inconsistent with the first-principles LSDA calculations, which reproduced reasonably well the experimental structural parameters.

The Pu_2MGa_8 compounds are not superconducting down to 2 K. In this respect, the strong analogy existing between the Ce-115 and Ce-218 superconductors is not continued in the Pu-115 and 218 families of compounds, and hence, PuCoGa_5 and PuRhGa_5 remain unique Pu-based superconductors. The origin of this difference between the Ce and Pu analogs is not easily pinpointed. Our calculations show that the Fermi surfaces of the Pu-218's are sufficiently different from those of the Pu-115's. Compared to the Ce analogs, this happens because the Pu $5f$ bands are more delocalized and dispersive than the more localized and narrower Ce $4f$ bands.

For the uranium 218 compounds we observe that the LSDA, delocalized $5f$ approach reproduces well the experimental data. We obtained, in agreement with experiment, a nonmagnetic ground state and the structural parameters are well described. The densities of states of the studied uranium 218 compounds were calculated and their band structures and Fermi surface topologies were analyzed. U_2CoGa_8 and U_2RhGa_8 are predicted to have three Fermi surface sheets, whereas four Fermi surface sheets are predicted for U_2FeGa_8 and U_2RuGa_8 . For each compound at least one of the sheets has a three-dimensional character.

The closely related Np_2CoGa_8 is predicted to have a magnetically ordered ground state. Our calculations predict an essentially localized state for Am_2CoGa_8 . An account of the f -electron localization, an electronic structure very similar to the related Ce-218 systems is obtained, which is also reflected in the similarity of their Fermi surfaces. The basic characteristics of the crystallographic, electronic, and magnetic structures of actinide 218 compounds obtained here are expected to be of a great value for future studies of this intriguing (and so far underexplored) class of compounds.

ACKNOWLEDGMENTS

We thank F. Wastin, R. Jardin, and D. Aoki for a valuable exchange of information and assistance in preparation and measurement of the 218 compounds. The high-purity Np and Pu metals required for the fabrication of the compounds were made available through a loan agreement between Lawrence Livermore National Laboratory (LLNL) and ITU, in the framework of a collaboration involving LLNL, Los Alamos National Laboratory, and the U.S. Department of Energy. N.M. acknowledges the European Commission for support given in the frame of the program Training and Mobility of Researchers. Support from the Swedish Research Council (VR), the Swedish National Infrastructure for Computing (SNIC), and from the Institute of Transuranium Elements through Contract No. 207146-2007-02 is also gratefully acknowledged.

*On leave from Faculty of Science, Menoufia University, Shebin El-kom, Egypt.

¹J. L. Sarrao, L. A. Morales, J. D. Thompson, B. L. Scott, G. R. Stewart, F. Wastin, J. Rebizant, P. Boulet, E. Colineau, and G. H. Lander, *Nature (London)* **420**, 297 (2002).

²N. J. Curro, T. Caldwell, E. D. Bauer, L. A. Morales, M. J. Graf, Y. Bang, A. V. Balatsky, J. D. Thompson, and J. L. Sarrao, *Nature (London)* **434**, 622 (2005).

³F. Wastin, P. Boulet, J. Rebizant, E. Colineau, and G. H. Lander, *J. Phys.: Condens. Matter* **15**, S2279 (2003).

- ⁴J. J. Joyce, J. M. Wills, T. Durakiewicz, M. T. Butterfield, E. Guziwicz, J. L. Sarrao, L. A. Morales, A. J. Arko, and O. Eriksson, *Phys. Rev. Lett.* **91**, 176401 (2003).
- ⁵E. D. Bauer, J. D. Thompson, J. L. Sarrao, L. A. Morales, F. Wastin, J. Rebizant, J. C. Griveau, P. Javorský, P. Boulet, E. Colineau, G. H. Lander, and G. R. Stewart, *Phys. Rev. Lett.* **93**, 147005 (2004).
- ⁶H. Sakai, Y. Tokunaga, T. Fujimoto, S. Kambe, R. E. Walstedt, H. Yasuoka, D. Aoki, Y. Homma, E. Yamamoto, A. Nakamura, Y. Shiokawa, K. Nakajima, Y. Arai, T. D. Matsuda, Y. Haga, and Y. Ōnuki, *J. Phys. Soc. Jpn.* **74**, 1710 (2005).
- ⁷N. Metoki, K. Kaneko, E. Colineau, P. Javorský, D. Aoki, Y. Homma, P. Boulet, F. Wastin, Y. Shiokawa, N. Bernhoeft, E. Yamamoto, Y. Onuki, J. Rebizant, and G. H. Lander, *Phys. Rev. B* **72**, 014460 (2005).
- ⁸P. S. Normile, S. Heathman, M. Idiri, P. Boulet, J. Rebizant, F. Wastin, G. H. Lander, T. Le Bihan, and A. Lindbaum, *Phys. Rev. B* **72**, 184508 (2005).
- ⁹S. Raymond, P. Piekarczyk, J. P. Sanchez, J. Serrano, M. Krisch, B. Janoušová, J. Rebizant, N. Metoki, K. Kaneko, P. T. Jochym, A. M. Olés, and K. Parlinski, *Phys. Rev. Lett.* **96**, 237003 (2006).
- ¹⁰I. Opahle, S. Elgazzar, V. D. P. Servedio, M. Richter, and P. M. Oppeneer, *EPL* **74**, 124 (2006).
- ¹¹N. Magnani, A. Hiess, R. Caciuffo, E. Colineau, F. Wastin, J. Rebizant, and G. H. Lander, *Phys. Rev. B* **76**, 100404(R) (2007).
- ¹²A. Hiess, A. Stunault, E. Colineau, J. Rebizant, F. Wastin, R. Caciuffo, and G. H. Lander, *Phys. Rev. Lett.* **100**, 076403 (2008).
- ¹³T. Park, F. Ronning, H. Q. Yuan, M. B. Salamon, R. Movshovich, J. L. Sarrao, and J. D. Thompson, *Nature (London)* **440**, 65 (2006).
- ¹⁴Y. Bang, A. V. Balatsky, F. Wastin, and J. D. Thompson, *Phys. Rev. B* **70**, 104512 (2004).
- ¹⁵I. Opahle and P. M. Oppeneer, *Phys. Rev. Lett.* **90**, 157001 (2003).
- ¹⁶F. Jutier, G. A. Ummarino, J.-C. Griveau, F. Wastin, E. Colineau, J. Rebizant, N. Magnani, and R. Caciuffo, *Phys. Rev. B* **77**, 024521 (2008).
- ¹⁷Yu. N. Grin, P. Rogl, L. G. Akselrud, V. K. Pecharskii, and Ya. P. Yarmolyuk, *Russ. Metall.* **4**, 206 (1988).
- ¹⁸M. Schönert, S. Corsépius, E.-W. Scheidt, and G. R. Stewart, *J. Alloys Compd.* **224**, 108 (1995).
- ¹⁹S. Ikeda, T. Okubo, Y. Inada, Y. Tokiwa, K. Kaneko, T. D. Matsuda, E. Yamamoto, Y. Haga, and Y. Ōnuki, *J. Phys.: Condens. Matter* **15**, S2015 (2003).
- ²⁰R. Troć, Z. Bukowski, C. Sułkowski, J. A. Morkowski, A. Szajek, and G. Chełkowska, *Physica B* **359-361**, 1375 (2005).
- ²¹H. Hegger, C. Petrovic, E. G. Moshopoulou, M. F. Hundley, J. L. Sarrao, Z. Fisk, and J. D. Thompson, *Phys. Rev. Lett.* **84**, 4986 (2000).
- ²²C. Petrovic, R. Movshovich, M. Jaime, P. G. Pagliuso, M. F. Hundley, J. L. Sarrao, Z. Fisk, and J. D. Thompson, *EPL* **53**, 354 (2001).
- ²³C. Petrovic, P. G. Pagliuso, M. F. Hundley, R. Movshovich, J. L. Sarrao, J. D. Thompson, Z. Fisk, and P. Monthoux, *J. Phys.: Condens. Matter* **13**, L337 (2001).
- ²⁴G.-q. Zheng, K. Tanabe, T. Mito, S. Kawasaki, Y. Kitaoka, D. Aoki, Y. Haga, and Y. Ōnuki, *Phys. Rev. Lett.* **86**, 4664 (2001).
- ²⁵Y. Kohori, Y. Yamato, Y. Iwamoto, T. Kohara, E. D. Bauer, M. B. Maple, and J. L. Sarrao, *Phys. Rev. B* **64**, 134526 (2001).
- ²⁶K. Izawa, H. Yamaguchi, Y. Matsuda, H. Shishido, R. Settai, and Y. Ōnuki, *Phys. Rev. Lett.* **87**, 057002 (2001).
- ²⁷T. Maehira, T. Hotta, K. Ueda, and A. Hasegawa, *Phys. Rev. Lett.* **90**, 207007 (2003).
- ²⁸J. D. Thompson, T. Park, N. J. Curro, F. Ronning, R. Movshovich, E. D. Bauer, and J. L. Sarrao, *J. Magn. Magn. Mater.* **310**, 532 (2007).
- ²⁹L. D. Pham, T. Park, S. Maquilon, J. D. Thompson, and Z. Fisk, *Phys. Rev. Lett.* **97**, 056404 (2006).
- ³⁰J. L. Sarrao and J. D. Thompson, *J. Phys. Soc. Jpn.* **76**, 051013 (2007).
- ³¹G. F. Chen, S. Ohara, M. Hedo, Y. Uwatoko, K. Saito, M. Sorai, and I. Sakamoto, *J. Phys. Soc. Jpn.* **71**, 2836 (2002).
- ³²M. Nicklas, V. A. Sidorov, H. A. Borges, P. G. Pagliuso, C. Petrovic, Z. Fisk, J. L. Sarrao, and J. D. Thompson, *Phys. Rev. B* **67**, 020506(R) (2003).
- ³³E. G. Moshopoulou, Z. Fisk, J. L. Sarrao, and J. D. Thompson, *J. Solid State Chem.* **158**, 25 (2001).
- ³⁴G. Amoretti and J. M. Fournier, *J. Magn. Magn. Mater.* **43**, L217 (1984).
- ³⁵P. M. Oppeneer, T. Kraft, and M. S. S. Brooks, *Phys. Rev. B* **61**, 12825 (2000).
- ³⁶L. V. Pourovskii, M. I. Katsnelson, and A. I. Lichtenstein, *Phys. Rev. B* **72**, 115106 (2005).
- ³⁷A. O. Shorikov, A. V. Lukoyanov, M. A. Korotin, and V. I. Anisimov, *Phys. Rev. B* **72**, 024458 (2005).
- ³⁸E. S. R. Gopal, *Specific Heats at Low Temperatures* (Plenum Press, New York, 1966).
- ³⁹P. Boulet, D. Bouxière, J. Rebizant, E. Colineau, and F. Wastin, in *Plutonium Futures—The Science*, edited by G. D. Jarvinen, AIP Conf. Proc. No. 673 (AIP, Melville, NY, 2003), pp. 136–138.
- ⁴⁰I. Opahle, Ph.D. thesis, University of Technology Dresden, 2001.
- ⁴¹H. Eschrig, M. Richter, and I. Opahle, in *Relativistic Electronic Structure Theory Part II: Applications*, edited by P. Schwerdtfeger (Elsevier, Amsterdam, 2004), pp. 723–776.
- ⁴²K. Koepernik and H. Eschrig, *Phys. Rev. B* **59**, 1743 (1999).
- ⁴³J. P. Perdew and Y. Wang, *Phys. Rev. B* **45**, 13244 (1992).
- ⁴⁴P. Blaha, K. Schwarz, G. K. H. Madsen, D. Kvasnicka, and J. Luitz, in *WIEN2k, An Augmented Plane Wave + Local Orbitals Program for Calculating Crystal Properties*, edited by Karlheinz Schwarz (Technische Universität Wien, Austria, 2001).
- ⁴⁵J. Kuneš, P. Novák, M. Diviš, and P. M. Oppeneer, *Phys. Rev. B* **63**, 205111 (2001).
- ⁴⁶J. Kuneš, P. Novák, R. Schmid, P. Blaha, and K. Schwarz, *Phys. Rev. B* **64**, 153102 (2001).
- ⁴⁷M. T. Czyżyk and G. A. Sawatzky, *Phys. Rev. B* **49**, 14211 (1994).
- ⁴⁸A. B. Shick, V. Drchal, and L. Havela, *EPL* **69**, 588 (2005).
- ⁴⁹A. B. Shick, V. Janiš, and P. M. Oppeneer, *Phys. Rev. Lett.* **94**, 016401 (2005).
- ⁵⁰A. Zelinskiy, A. Fedorchuk, O. Zelinska, and H. Noël, *Visnyk Lviv Univ. Ser. Chem.* **48**, 72 (2007).
- ⁵¹I. Opahle, S. Elgazzar, K. Koepernik, and P. M. Oppeneer, *Phys. Rev. B* **70**, 104504 (2004).
- ⁵²A. L. Cornelius, A. J. Arko, J. L. Sarrao, J. D. Thompson, M. F. Hundley, C. H. Booth, N. Harrison, and P. M. Oppeneer, *Phys. Rev. B* **59**, 14473 (1999).
- ⁵³M.-T. Suzuki and P. M. Oppeneer, *Phys. Rev. B* **80**, 161103(R)

- (2009).
- ⁵⁴P. M. Oppeneer, A. B. Shick, J. Ruzs, S. Lebègue, and O. Eriksson, *J. Alloys Compd.* **444-445**, 109 (2007).
- ⁵⁵G. Kotliar, S. Y. Savrasov, K. Haule, V. S. Oudovenko, O. Parcollet, and C. A. Marianetti, *Rev. Mod. Phys.* **78**, 865 (2006).
- ⁵⁶A. B. Shick, J. Kolorenč, A. I. Lichtenstein, and L. Havela, *Phys. Rev. B* **80**, 085106 (2009).
- ⁵⁷J. Ruzs, M. Biasini, and A. Czopnik, *Phys. Rev. Lett.* **93**, 156405 (2004).
- ⁵⁸M. Biasini, G. Ferro, and A. Czopnik, *Phys. Rev. B* **68**, 094513 (2003).
- ⁵⁹E. Colineau, P. Javorský, P. Boulet, F. Wastin, J.-C. Griveau, J. Rebizant, J. P. Sanchez, and G. R. Stewart, *Phys. Rev. B* **69**, 184411 (2004).
- ⁶⁰B. Detlefs, S. B. Wilkins, R. Caciuffo, J. A. Paixao, K. Kaneko, F. Honda, N. Metoki, N. Bernhoeft, J. Rebizant, and G. H. Lander, *Phys. Rev. B* **77**, 024425 (2008).
- ⁶¹T. Okane, T. Ohkochi, T. Inami, Y. Takeda, S.-i. Fujimori, N. Kawamura, M. Suzuki, S. Tsutsui, H. Yamagami, A. Fujimori, A. Tanaka, D. Aoki, Y. Homma, Y. Shiokawa, E. Yamamoto, Y. Haga, A. Nakamura, and Y. Ōnuki, *Phys. Rev. B* **80**, 104419 (2009).
- ⁶²Note also that these are calculated by two completely different electronic structure codes.
- ⁶³T. Ueda, H. Shishido, S. Hashimoto, T. Okubo, M. Yamada, Y. Inada, R. Settai, H. Harima, A. Galatanu, E. Yamamoto, N. Nakamura, K. Sugiyama, T. Takeuchi, K. Kindo, T. Namiki, Y. Aoki, H. Sato, and Y. Ōnuki, *J. Phys. Soc. Jpn.* **73**, 649 (2004).